Principle and Performance of a Dual-band Search Coil Magnetometer: a New Instrument to Investigate Fluctuating Magnetic Fields in Space[1]

C. Coillot, J. Moutoussamy, R. Lebourgeois, S. Ruocco, and G. Chanteur

Abstract—**Search-coil magnetometers are of common use in space physics thanks to their simplicity, robustness and ability to measure weak magnetic fields: their sensitivity can reach a few tens of fT/√Hz in the range 10-100kHz. The frequency band is grossly determined by the resonance of the coil. Simply adding a second coil does not efficiently extend the frequency band beyond the first resonance due to the mutual impedance of the two coils. We present a solution, called "mutual reducer", which allows to take full benefit of the second coil and efficiently extends the frequency band. The physical principle is described first, followed by a detailed presentation of this "dual-band search-coil" (DBSC) that will be part of the Plasma Wave Instrument (PWI) onboard the Mercury Magnetospheric Orbiter (MMO) of the ESA-JAXA mission BepiColombo dedicated to the exploration of the plasma environment of planet Mercury.**

Keywords—**Magnetometers, magnetic analysis, mutual coupling, frequency response.**

I. INTRODUCTION

Sensitive and accurate measurements of DC and fluctuating magnetic fields are mandatory to characterize plasma phenomena occurring in the interplanetary medium pervaded by the solar wind or in the vicinity of solar system objects (*i.e.* planets and their natural satellites, comets, asteroids, …) 1, 2. Usually, two kinds of magnetometers are embarked onboard scientific spacecraft aiming at measuring magnetic fields in space 3 : (i) fluxgates well adapted for weak magnetic fields from DC to a few Hz, (ii) search coils covering the frequency band from around [1]00

mHz up to a few kHz. The frequency dependent sensitivity of a magnetometer is characterized by the Noise Equivalent Magnetic Induction (*NEMI*) which is the smallest amplitude of an external harmonic magnetic induction at a frequency f which produces a detectable output signal above the noise level of the instrument at that frequency. For a fluxgate the *NEMI* is almost constant from DC up to a few tens of Hz, while it is V-shaped for a search coil as demonstrated in section IV. The two *NEMI* curves intersect at the crossover frequency f_{co}, with the fluxgate being more sensitive than the search coil below f_{co}, and the search coil performing better above f_{co}. Moreover, due to its decreasing *NEMI* the search coil is better adapted to detect natural electromagnetic waves as their power spectrum generally varies like f^{-a} with 1<a<5. As typical fluxgates used in space physics have a *NEMI* on the order of 10000fT/√Hz, the objective of this project was to design a search coil achieving a better *NEMI* above 1Hz.

For exploratory space missions of poorly known environments it is desirable to design instruments having large enough dynamics and frequency bands, meanwhile being compliant with allowed mass and energy budgets and various constraints due to the thermal or radiation conditions prevailing in the targeted environment. For the BepiColombo mission expected physical phenomena encompass electromagnetic waves of various origins. Magnetospheric electromagnetic waves are expected to be observed from very low frequencies below 1Hz, associated with heavy planetary ions (O+, Na+, K+ …), up to 10-20 kHz associated to auroral electron cyclotron radiation.

Despite the fact that high frequency synchrotron radiation by magnetospheric electrons at Mercury seems to be unlikely, considering the present understanding of the Hermean environment, there are electromagnetic waves up

C. Coillot, J. Moutoussamy, G. Chanteur, CNRS/LPP - 10-12, Avenue de l'Europe – F-78140 Vélizy –France (corresponding author is Christophe Coillot, phone: 33-1-39-25-48-58, email : christophe.coillot@lpp.polytechnique.fr)
S. Ruocco, CNRS/LATMOS, 10-12, Avenue de l'Europe – F-78140 Vélizy –France

R. Lebourgeois is with Thalès Research and Technology - Route Départementale 128 – 91767 Palaiseau - France
Digital Object Identifier :

An earlier version of this paper was presented at the 2007 IEEE Conference and was published in its proceedings

to a few 100kHz associated with solar bursts and planetary foreshock phenomena worth to investigate. These scientific objectives have motivated us to design a wide-band search-coil.[2] The increased complexity of its design is worth the effort considering the saving of mass and volume it allows compared to the use of two traditional sensors covering two overlapping frequency bands. This is an important issue for space applications.

II. BASICS OF SEARCH COIL

A regular search-coil consists of a conductor coiled around a magnetic core: Faraday's law of induction relates the voltage across the terminals of the coil to the rate of change of the magnetic flux through the coil. The magnetic flux through the coil is augmented by the presence of the magnetic core (4, 5), usually a cylinder: it has been shown in 6 that a drastic improvement of the magnetic amplification is achieved by using an optimized shape with flaring ends illustrated by 1. The sensor is connected to a very low noise preamplifier 7. In the case of voltage amplification a feedback loop is used in addition to flatten the natural resonance of the sensor 8. Current amplification is a possible alternative which does not require any feedback but slightly increases the power consumption.
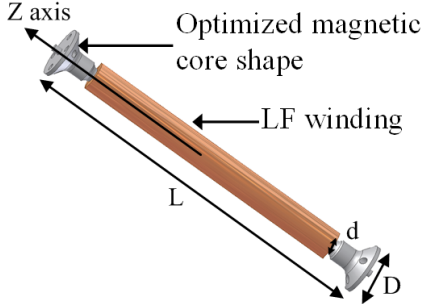

Fig. 1   Schematic view of the search coil sensor showing the low frequency coil wound around the optimized magnetic core consisting of a cylinder with added flaring extremities.

Let us first consider a sensor designed to reach 2000fT/√Hz at 10Hz with the following characteristics : optimized core with a relative permeability μ_r =2500, 100mm length, 4mm diameter, and 14000 turns. The transfer function of this low frequency (LF) search coil is depicted on 2. as well as its *NEMI* which first decreases with frequency, up to the resonance frequency f_{LF} around 2kHz, where it reaches its minimum of 40fT/√Hz, and increases beyond. This sensor is well fitted for magnetic measurements in the low and intermediate frequency ranges below 20kHz, but a priori not enough sensitive for detecting weak magnetic fluctuations in the 100kHz frequency domain.
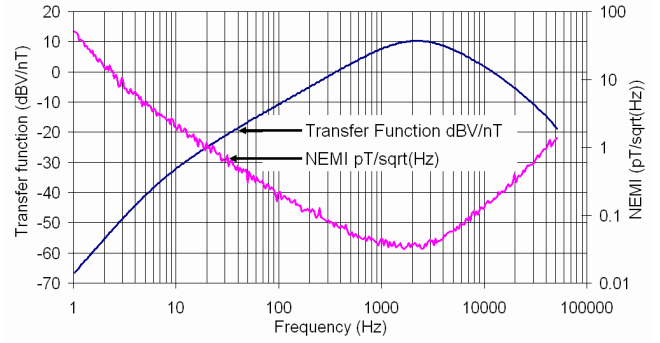
Fig. 2   Transfer function and *NEMI* curve of the low frequency search coil between 1Hz and 100kHz, with their respective scales on the left and right sides of the plots.

III. ROUGH MODELING OF THE MAGNETIC CORE

First, we propose the following way to estimate the magnetic amplification of a cylinder with flaring ends, as represented on 1.

When a magnetic body is immersed into a magnetic field H_{ext} a magnetization appears and the internal field is given by $H_{int} = H_{ext} - NM$ where N is the demagnetizing factor and M the magnetization. The demagnetizing factor N depends upon the shape and orientation of the magnetic body with respect to the external field. With a few exceptions like the ellipsoid 4, the cylinder ([5], [9]) and the rectangular prism 10, N is generally a tensor depending upon coordinates and numerical computations are necessary to estimate the demagnetizing field $H_d = -NM$ even when the external field H_{ext} is uniform as supposed in the present study. The magnetic flux density, or magnetic induction, B inside the body is linked to the magnetic field by $B = \mu_r H_{int}$, where μ_r denotes the relative permeability of the magnetic material, related to the magnetic susceptibility χ_r by $\chi_r = \mu_r - 1$. The ratio $B/\mu_0 H_{ext}$, called the apparent permeability μ_{app}, can be computed from the relative permeability μ_r of the magnetic material and the demagnetizing factor N. We make two rough assumptions: the demagnetizing factor N reduces to a scalar, its component N_Z along the measurement axis z, which is constant throughout the whole core (cf. Fig.1). That leads to the following apparent permeability μ_{app}:

$$\mu_{app} = \frac{B}{\mu_0 H_{ext}} = \frac{\mu_r}{1 + (\mu_r - 1) N_z} \qquad (1)$$

A long cylinder of length L and diameter d however, made of a high permeability material, can be roughly approximated by an oblate ellipsoid, leading to the following approximate demagnetizing factor along the z axis:

$$N_Z(m) = \frac{1}{m^2 - 1} \left[\frac{m}{\sqrt{m^2 - 1}} \ln(m + \sqrt{m^2 - 1}) - 1 \right] \qquad (2)$$

where $m=L/d\gg1$ denotes the aspect ratio of the cylinder. Let us now express the demagnetizing field for the magnetic core of length L with flaring ends of diameter D ("diabolo" core) and the one of a cylinder of length L and diameter D as:

-   Cylinder: $H_d = -N_Z(L/D)M$ and $M = \chi H$

-   Diabolo: $H_d' = -N_Z'(L/D)M'$ and $M' = \chi H'$

By noticing that the cylinder and the diabolo have the same surface density of magnetic poles at their ends, we deduce that their related demagnetizing magnetic fields are identical at the ends of the core:

$$H_d' = H_d \qquad (3)$$

Then, we compute the magnetic field at the centre of the diabolo core (H') of diameter d' by means of the flux conservation between the ends and the centre of the diabolo core as:

$$H = \frac{d'^2}{D^2} H' \qquad (4)$$

and,

$$\begin{aligned} H' &= H_{ext} + H_d' \\ &= H_{ext} + H_d \end{aligned} \qquad (5)$$

By replacing, H_d in (5) we express:

$$H' = H_{ext} - N_Z(L/D)\chi H \qquad (6)$$

By replacing H from (4) in (6) we obtain :

$$H' = H_{ext} - N_Z(L/D)\chi \frac{d'^2}{D^2} H' \qquad (7)$$

This leads to:

$$\frac{H'}{H_{ext}} = \left(1 + N_Z(L/D)\chi \frac{d'^2}{D^2}\right)^{-1} \qquad (8)$$

Finally, we obtain:

$$\mu_{app} = \frac{B'}{\mu_0 H_{ext}} = \frac{\mu_r}{1 + (\mu_r - 1)N_Z(L/D)\dfrac{d'^2}{D^2}} \qquad (9)$$

The accuracy of this formula has been compared with simulations carried out with the finite element software Flux2D. This model fits with simulations within 10% for diameter ratios $1<D/d'<5$. The diabolo shape increases considerably the apparent permeability μ_{app} at the center of the magnetic core 6.

IV.   DISCUSSION OF THE FREQUENCY BEHAVIOR

A harmonic external magnetic induction $Be^{j\omega t}$ of amplitude B and pulsation ω induces a voltage $V(t)$ of amplitude V between the terminals of the winding:

$$V(t) = -\frac{d\varphi(t)}{dt} \quad , \quad V = N_1 S \mu_{app} \omega B \qquad (10)$$

where $\varphi(t)$ is the magnetic flux through the N_1 turns of the coil, S is the sectional area of the core, μ_{app} is the apparent permeability of the core approximated by (9).

We assume that the sensor is equivalent to the RLC circuit displayed by Fig. 3, where L_1 is the inductance of the winding, R_1 its electrical resistance, and C_1 its capacitance. Thus, the transfer function between the output voltage V_{OUT} and the external magnetic field is equal to:

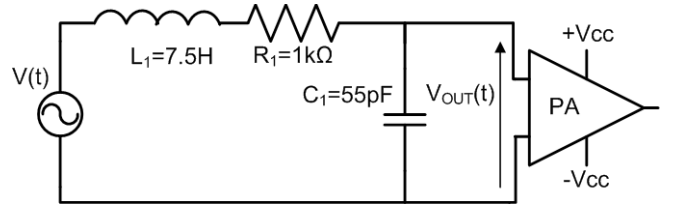$$T(j\omega) = \frac{V_{OUT}}{B_{ext}} = \frac{-j\omega N_1 S \mu_{app}}{(1 - L_1 C_1 \omega^2) + jR_1 C_1 \omega}$$

Fig. 3   Equivalent electrical circuit of the search coil: e(t) is the voltage induced by the varying external magnetic induction, L_1 is the inductance of the coil, R_1 its resistance , and C_1 its capacitance. The output voltage V_{OUT} of the sensor is applied to a preamplifier having a high input impedance.

The detection threshold per Hertz of the output voltage is equal to the square root of the variance per Hertz v^2_{noise} of the noise voltage of the sensor given by:

$$v^2_{noise} = v^2_{PA} + 4kTR_1 \qquad (11)$$

where v^2_{PA} is the variance per Hertz of the noise voltage at the entry of the preamplifier, and $4kTR_1$ is the variance per Hertz of the thermal noise voltage of the resistance, where $k=1,38\times10^{-23}J.K^{-1}$ is the Boltzmann constant and T the temperature.

Hence the *NEMI*, defined as the smallest magnetic induction B which can be detected due to the noise of the sensor, is the following V-shaped function of ω :

$$NEMI = \frac{\sqrt{v_{PA}^2 + 4kTR_1}}{N_1 S \mu_{app} \omega} \sqrt{(1 - L_1 C_1 \omega^2)^2 + (R_1 C_1 \omega)^2} \quad (12)$$

At low frequencies, the *NEMI* decreases with frequency and is approximated by the following formula, which does not involve the resonance frequency:

$$NEMI = \frac{\sqrt{v_{PA}^2 + 4kTR_1}}{N_1 S \mu_{app} \omega} \qquad (13)$$

This simple expression can be used to estimate the number of turns N_1 required to achieve a targeted value of the *NEMI* at a given frequency much smaller than the resonance frequency (in the present case 2000fT/√(Hz) at 10Hz): let us nevertheless notice that R_1 is proportional to N_1. More modeling details are given in 7 and 8 especially with respect to the effect of the flux-feedback which is not taken into account in the present qualitative discussion.

V. FEASIBILITY OF A WIDE BAND SEARCH COIL USING TWO WINDINGS ON A UNIQUE MAGNETIC CORE

The designed LF coil is not enough sensitive to detect natural waves at frequencies larger than a few tens of kHz. An obvious idea to extend the frequency range of measurements up to 1MHz is to implement a second winding with a higher resonance frequency f_{HF} of the order of 300kHz. The transition frequency f_{tr} between the two bands, defined by the intersection of the LF and HF *NEMI*s, is chosen equal to 10kHz. Let us first consider the frequency band [1Hz, 10kHz] covered by the LF coil; accordingly to Fig.2 the LF-NEMI at 10kHz is equal to 100fT/√Hz, which is also the value of the LF-NEMI at $f_1 \sim 200$Hz in the validity range of formula (13).Then, in order to design a HF coil operating in the frequency band [10kHz, 1MHz], and having a *HF-NEMI* equal to the *LF-NEMI* at the transition frequency f_{tr} =10kHz, we make use of an expression similar to (13) as f_{tr} is much smaller than f_{HF}. Considering the same magnetic core, and assuming the same noise level at the entry of the preamplifier, we can express the number of turns of the HF coil from the number of turns of the LF coil, multiplied by the ratio of the two frequencies:

$$N_2 \approx N_1 \frac{f_1}{f_{tr}} \approx \frac{N_1}{50} \qquad (15)$$

When a HF coil with N_2 =280 turns is wound all alone on a magnetic core (Ferrite diabolo core: L=100mm, D=14mm, d=4mm), its transfer function is the expected one: the gain increases with frequency up to the resonance frequency f_{HF}, slightly above 300kHz, and decreases beyond due to the capacitive behavior of the coil as shown by the curve labeled HF1 in Fig.4. But when the same HF coil is wound over the LF coil, together on the same magnetic core, the transfer function represented by curve HF2 on Fig.4 exhibits a pair of resonance and anti-resonance at ~6 and ~18kHz, above the resonance frequency f_{LF} of the LF coil. The gain increases with frequency beyond the anti-resonance but remains roughly 20dB below the HF1 gain.
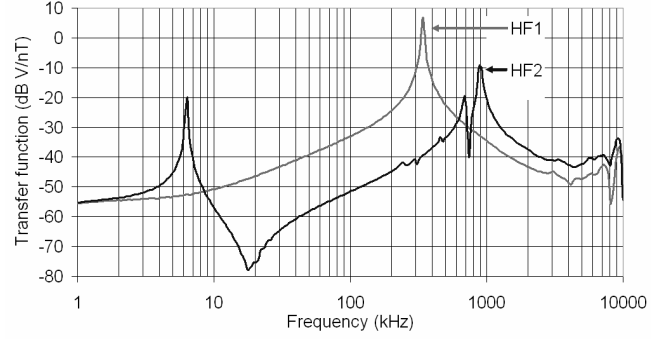

Fig. 4   Transfer functions of the HF winding: (i) all alone on a magnetic core (HF1), and (ii) together with the LF winding (HF2) on the same magnetic core.

In order to explain qualitatively this behavior let us consider the magnetic flux ϕ through each coil;

$$\phi_1 = N_1 S \mu_{app} B + L_1 I_1 + M_{21} I_2 \qquad (16)$$

$$\phi_2 = N_2 S \mu_{app} B + L_2 I_2 + M_{12} I_1 \qquad (17)$$

where indices 1 and 2 relate respectively to the LF and HF windings, and symbols L and M denote the self and mutual inductances.

At frequencies lower than the HF resonance frequency f_{HF} the current intensity I_1 flowing through the LF coil is not much influenced by the magnetic coupling with the HF coil and is approximately given by:

$$I_1 = -\frac{N_1 S \mu_{app} B j \omega}{R_1 + j L_1 \omega + 1/(j C_1 \omega)} \qquad (18)$$

At frequencies lower than the LF resonance frequency f_{LF} this current is small. At frequencies larger than f_{LF} the main contribution to the impedance of the LF winding comes from the inductive part $j L_1 \omega$ and I_1 is further approximated by:

$$I_1 \approx -\frac{N_1 S \mu_{app} B}{L_1} \text{ for } 1/\sqrt{L_2 C_2} > \omega > 1/\sqrt{L_1 C_1}. \qquad (19)$$

Substituting approximation (19) into equation (17) gives:

$$\phi_2 = N_2 S \mu_{app} B + L_2 I_2 - M_{12} \frac{N_1 S \mu_{app} B}{L_1} \qquad (20)$$

$$\phi_2 = (1 - \sigma_{12}) N_2 S \mu_{app} B + L_2 I_2 \qquad (21)$$

where σ_{12} is the mutual coupling coefficient between the two windings. When, the windings are implemented on a unique magnetic core, this coefficient σ_{12} is close to 1 and the latter expression is almost independent of the external magnetic induction. Thus a HF coil wound directly over the LF coil, together on the same magnetic core, is inefficient to

measure the external magnetic induction in the frequency range [f_{LF} , f_{HF}].

VI. PHYSICAL DESCRIPTION OF A MUTUAL REDUCER

It is therefore mandatory to reduce the mutual coupling between the LF and HF coils wound together on the same magnetic core in order to extend the frequency range of measurements. The original solution we propose consists in inserting a tubular magnetic shield between the two windings as shown by 5. This shield offers a new path to the self-induction flux of the LF winding (red lines on 6), which results in a considerable decrease of the LF self-induction flux seen by the HF winding, hence the name "mutual reducer".
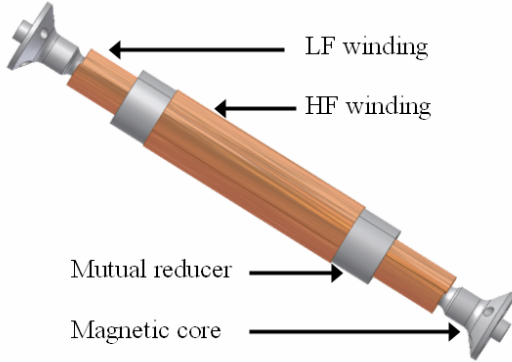

Fig. 5   The dual-band search coil magnetometer consists of two coils wound on the same magnetic core and separated by a tubular magnetic shield reducing the mutual coupling of the two coils.

Then the magnetic parts of the LF and HF coils have different apparent permeabilities, μ_{app1} and μ_{app2} respectively, which depend upon the shapes and cross-sectional areas of the magnetic core and mutual reducer. The various parameters of the sensor: auto and mutual inductions, and apparent permeabilities, are obtained via numerical computation. The flux through the HF winding can be written:

$$\phi_2 = N_2 S_2 \mu_{app2} B + L_2 I_2 - M_{12} \frac{N_1 S_1 \mu_{app1} B}{L_1} \qquad (23)$$

where S_1 is the cross-sectional area of the core, and S_2 denotes the sum of the cross-sectional areas of the core and the reducer. ϕ_2 can be written:

$$\phi_2 = \mu_{app2}^* N_2 S_2 B + L_2 I_2 \qquad (24)$$

$$\mu_{app2}^* = \mu_{app2} - \frac{M_{12}}{L_1} \frac{N_1}{N_2} \frac{S_1}{S_2} \mu_{app1} \qquad (25)$$

where μ_{app2}^* is the apparent permeability for the HF coil reduced by the mutual coupling to the LF coil. The coupling must be as low as possible in order to keep this reduced apparent permeability as large as possible. Fig. 6 shows that part of the LF auto-induction flux is captured by the mutual reducer, and thus the HF coil feels only the remaining part of this LF flux.

The measured transfer function for an HF winding combined with a mutual reducer is presented on 7 (curve labelled HF3). The HF3 curve is close to the transfer function HF1 of the HF coil wound all alone on the magnetic core. However a remaining mutual coupling with the LF winding is revealed by a resonance occurring at about 5 kHz followed by an anti-resonance at about 6kHz. The resonance clearly originates from the coupling to the LF winding, while the anti-resonance is supposed to result from the energy exchange between the capacitance of the LF winding and the mutual-inductance.
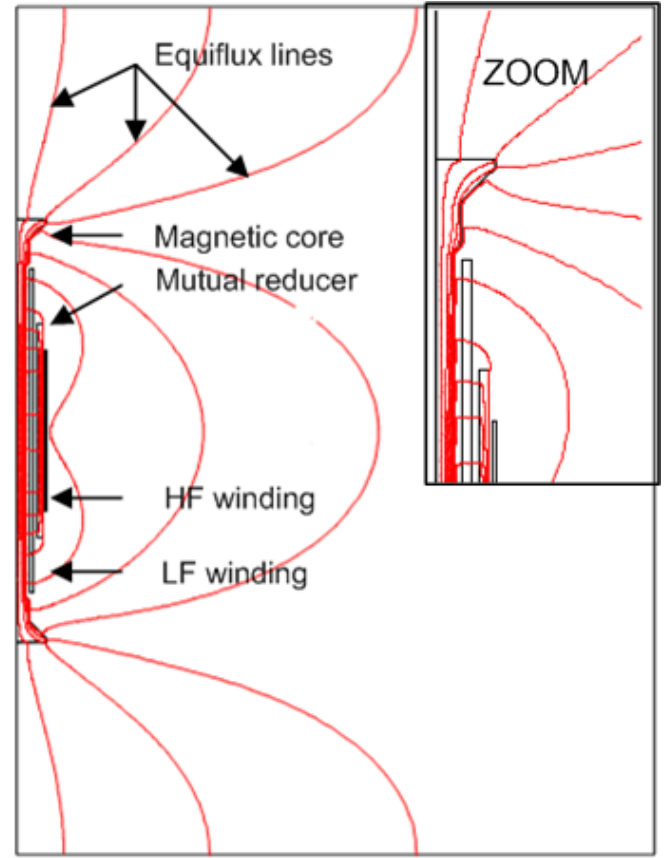

Fig. 6   Field lines of the magnetic induction modified by the mutual reducer which captures a fraction of the return auto-induction flux created by the LF coil and guides it inside the HF coil.

This assertion is motivated by the comparison of Fig. 4 and Fig. 7: the anti-resonance frequency decreases when the

mutual coupling decreases. The abrupt variation of HF3 between 5 and 6kHz on Fig. 7 is due to the close proximity of the resonance and anti-resonance when the mutual reducer is added. The achieved HF transfer function makes possible the measurement of weak magnetic fields between 10kHz and 1MHz.
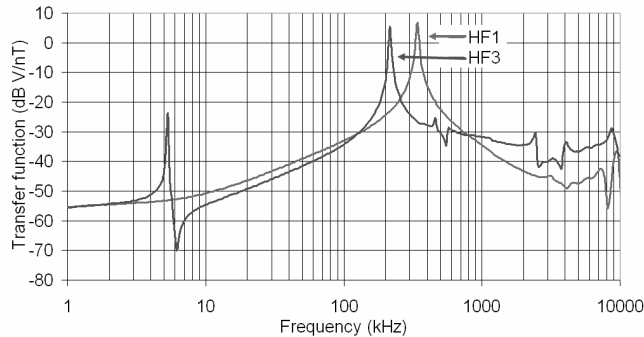

Fig. 7   Transfer function for of the HF coil wound all alone on the magnetic core (HF1), and transfer function of the HF coil wound together with the LF coil on the magnetic core, and combined with a mutual reducer (HF3).

VII.   PERFORMANCES OF THE DUAL-BAND SEARCH-COIL MAGNETOMETER

Thalès Research and Technology has designed several ferrite materials that keep a high magnetic permeability in the stringent temperature range [-100°C, 200°C] that will be met during the BepiColombo mission. The Mn-Zn ferrite selected for the dual-band search-coil has a relative permeability higher than 1000 on the full temperature range 11. The apparent permeability of the core for the LF coil is reduced from 295 to 265 when the mutual reducer is inserted, meanwhile the apparent permeability of the HF winding increases from almost 0 to 24, a value slightly larger than the apparent permeability for the HF coil when it is wound all alone on the magnetic core. The 10% loss of apparent permeability that affects the LF coil performance is compensated for by an almost proportional increase of the number of turns N_1. Each winding of the sensor is connected to its own low noise preamplifier. A first amplification stage involving a JFET is well suited for a high impedance sensor, and is used in order to minimize the contribution to the shot noise. The output noise can be written, similarly to (11):

$$V_{out}^2 = G_v^2 \left(V_{PA}^2 + 4kTR_1 \right)$$ (25)

where G_V represents the voltage gain of the preamplifier.

A flux feedback is used to flatten the transfer function of search coil around its resonance: the principle of this flux-feedback is detailed in 12. The transfer function of the LF coil with the flux-feedback has been presented in section II. The bloc diagram on 8 shows schematically how the output of each preamplifier is connected to a secondary coil in serial

with a feedback resistor R_{fb} in order to create a feedback flux. Hence the electronic noise is fed into the sensor and produces the following noise (26) which is added to the measured magnetic induction:

$$B_{fb} = \frac{M_{fb}}{S_1} \frac{v_{out}}{R_{fb}}$$ (26)

where M_{fb} is the mutual inductance between the main coil and the feedback coil. The resulting NEMI with the feedback is thus given by:

$$NEMI^2 = \left(NEMI_0^2 + B_{fb}^2 \right)$$ (26)

where $NEMI_0$ is the *NEMI* defined by (12).

The current source used for the LF flux feedback entails a wide band noise which has to be low-pass filtered in order to get the lowest possible *NEMI* in the HF frequency range. The coil used for the feedback also allows to inject into the sensor the magnetic flux created by an external signal in order to calibrate the instrument in flight.
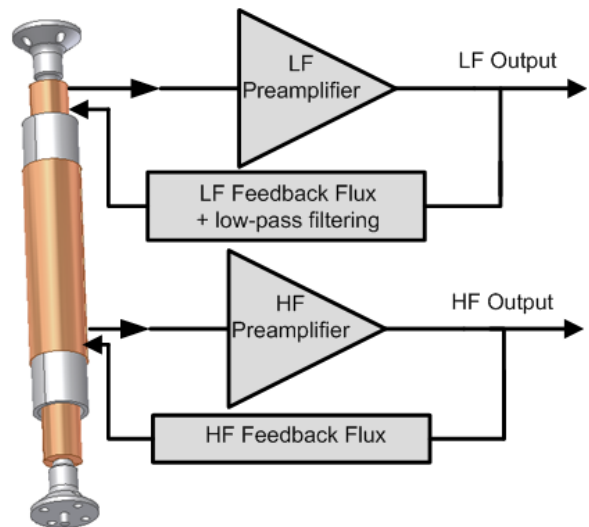

Fig. 8   Bloc diagram of the dual band search coil magnetometer.

The *NEMI* curves (in fT/√(Hz)) of the Bepicolombo dual-band search-coil, including the effect of the flux-feedback, are represented on 9. The *LF-NEMI* is plotted from 1Hz to 50kHz, and the *HF-NEMI* from 10kHz to 1MHz. The *DBSC-NEMI* defined as the minimum of the LF and HF *NEMIs* is lower than *NEMIs* of other sensors in comparable frequency ranges reported in the literature 13. Measurement have been performed at the Magnetic Observatory at Chambon la Forêt (France), which is a very quiet place for magnetic measurements, free from man-made magnetic perturbations.
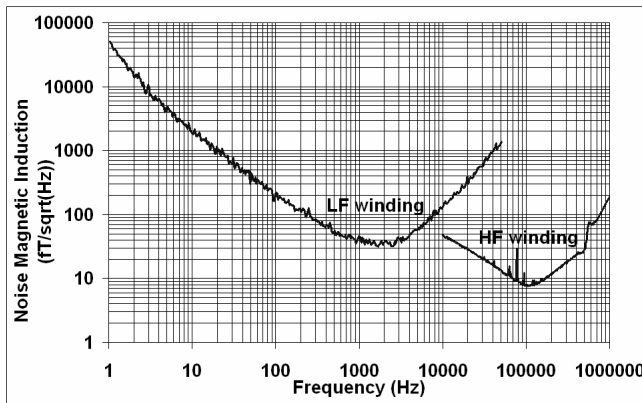
Fig. 9   NEMI curve of the Bepicolombo dual-band search coil magnetometer.

The designed sensor has a *NEMI* of 2000fT/√Hz at 10Hz, lower than 50fT/√Hz from 500 Hz to 500kHz, with a minimal value equal to 7,5fT/√Hz at 100kHz. These performances are among the best known for this family of magnetic sensors. However let us mention that an abrupt variation of the transfer function appears above 500kHz. This behaviour is still unexplained but seems to be linked to a LF resonance seen by the HF winding. Further investigations will be led to understand the origin of this resonance.

VIII.   CONCLUSION

The Dual Band Search-Coil (DBSC) is a good alternative to the use of two distinct sensors in applications where mass and volume are limited as for example for onboard instrumentation. When two different sensors are used they should be separated by a distance at least of the same order as their size, which means that the mechanical structure needed to hold the sensors would have a larger mass. The implementation of the mutual reducer described in this article allows to build a DBSC able to measure magnetic field fluctuations from 0.1Hz up to 1MHz. The DBSC designed for BepiColombo/MMO is 10cm long, 17mm in diameter, weighs 60g, and has an upper cut-off frequency of 640 kHz imposed by the high frequency receiver used [14]. The DBSC is associated with two classical search coils, designed at Kanazawa University, to form a tri-axial AC magnetometer which is part of the Plasma Wave Instrument of the MMO spacecraft [14]. The DBSC is aligned with the spin axis of the spacecraft, while the two identical classical search coils are lying in the spin plane.

ACKNOWLEDGMENT S

REFERENCES

[1]   F.F. Chen, "Introduction to plasma physics", 2nd Edition, Plenum press, 1984.

[2]   **N.** Cornilleau-Wehrlin et al., "First results obtained by the Cluster STAFF experiment", *Annales Geophysicae*, **21**, pp 437-456, 2003.

[3]   P. Ripka, "Magnetic sensors and magnetometers", Edition Artech house-Norwood, pp. 57-65, 2001.

[4]   J.A. Osborn, "Demagnetizing factors of the general ellipsoids", Physical Review, Vol 67, pp. 351-357, June 1945.

[5]   R.M. Bozorth, D.M. Chapin, "Demagnetizing factor of rods", Journal of applied physics, n°13, pp 320-327, May 1942.

[6]   C. Coillot, J. Moutoussamy, P. Leroy, G. Chanteur, A. Roux, "Improvements on the design of search coil magnetometer for space experiments", sensor letters, Vol 5, N° 1, pp 167-170, March 2007.

[7]   D.G. Lukoschus, "Optimization theory for induction-coil magnetometers at higher frequencies", IEEE Transactions on geoscience electronics, Vol GE-17, n°3, pp56-63, July 1979.

[8]   H.C. Seran, P. Fergeau, "An optimized low frequency three axis search coil for space research", Review of Scientific Instruments, Vol 76, Issue 4, pp 44502-1 – 44502-10, 2005.

[9]   Du-Xing Chen, James A. Brug, "Demagnetizing Factors for Cylinders", IEEE Transactions on magnetics, Vol 27, n°4, pp3601-3619, July 1991.

[10] A. Aharoni, "Demagnetizing factors for rectangular ferromagnetic prisms", Journal of applied physics, Vol 83, n°6, pp 3432-3434, March 1998.

[11] R. Lebourgeois, C. Coillot, "Mn-Zn ferrites for magnetic sensor in space applications", Journal of Applied Physics, Vol 103, March 2008.

[12] S. Tumanski, "Induction coil sensors-a review", Measurelent Science and Technology, Vol 18, Issue 3, March 2007.

[13] R.J. Prance, T.D. Clark, H. Prance, "Ultra low noise induction magnetometer for variable temperature operation", Sensosrs and Actuators, vol. 85, pp 361-364, 2000

[14] Y. Kasaba, J.-L. Bougeret, L.G. Blomberg, H. Kojima, S. Yagitani, M. Moncuquet, J.-G. Trotignon, G. Chanteur, A. Kumamoto, Y. Kasahara, J. Lichtenberger, Y. Omura, K. Ishisakai, H. Matsumoto, The Plasma Wave Investigation (PWI) onboard the BepiColombo/MMO: First measurement of electric fields, electromagnetic waves, and radio waves around Mercury. Planet. Space Sci. (2008), doi:10.1016/ j.pss.2008.07.017

C. Coillot (photograph not available at time of publication) was born in Choisy le Roi, France, in 1971, and graduated in electrical engineering from Ecole Normale Supérieure de Cachan in 1996. He received the PhD degree in electronics from the University of Montpellier, France, in 1999.
From 1999 to 2000, he worked as TEACHER of electrical engineering in technical school. From 2000 to 2001, he worked as electronic ENGINNER at Alcatel-Optronics.
In 2001, he joined the LPP (Laboratory of Plasma Physics, ex-part of CETP) as Research Engineer to manage magnetometer instrument design for spatial experiments and to conduct the research activity of LPP in magnetometry. His field of interest concerns high sensitivity magnetometers for space purpose. He has studied low noise electronic,

search coil modelling and optimization. He is currently involved in spacecraft experiments: Bepicolombo for Mercury environment and MMS for Earth environment. He is author or co-author of 7 publications in refereed journals.

J. Moutoussamy (photograph not available at time of publication) was born in Basse-Terre, Guadeloupe, France, in 1970. He is a full time teacher since 1996 at Dijon technological high school, G. Eiffel. He teaches object-oriented programming, instrumentation and real-time systems in undergraduate technical classes. In 2003, he joined the LPP, Velizy, France, to pursue his PhD degree on wide band magnetometers and giant magnetoimpedance transducers for space-oriented applications.

S. Ruocco (photograph not available at time of publication) was born in 1980 in Avignon (France). He received the advanced vocational diploma of Philippe de Girard high school (Avignon) in 1999. He joined the LATMOS in 2002. He is currently involved in low noise preamplifier on Bepicolombo spacecraft and technical manager of the low frequency receiver of TARANIS spacecraft.

R. Lebourgeois (photograph not available at time of publication) was born in 1962 in Montreuil-sous-Bois (France). He received the Engineering degree of the "Ecole Nationale Supérieure d'Ingénieur Electricien de Grenoble" (Polytechnic Institute of Grenoble) in 1986 and a Ph.D in Material Science at the Polytechnic Institute of Grenoble in 1989. He joined the Central Research Laboratory of THOMSON-CSF (now THALES Research & Technology) in October 1989. He made a lot of works and published a lot of papers on Ferrites and magnetic materials for power electronics. He is in charge of the studies related to Magnetic Materials, Ferrites and Dielectrics at THALES Research & Technology.

G. Chanteur (photograph not available at time of publication) was born in Lyon, in 1949, and graduated in physics from Ecole Normale Supérieure de Saint Cloud in 1974(N.B. ENS Saint Cloud is now known as ENS Lyon after it moved there).
Working in space physics since 1975 he has studied instabilities and solitary waves in plasmas. Involved in numerical simulation of space plasmas he has done particle in cell, MHD and hybrid simulations. Co-I of the CLUSTER/STAFF experiment he has designed theoretical methods of data analysis for multi-spacecraft missions. Since 1998 he has started activities in planetary physics both as Co-I on BepiColombo/MMO and as computer physicist designing three-dimensional hybrid simulation models for the global plasma environment of small planets.
Senior scientist at CNRS since 1997 he is author or co-author of about 50 publications in refereed journals. He has been lecturing computational methods at Versailles University and supervised 3 PhD thesis in space plasma physics and applied mathematics.